Program Digest, 2019 IEEE International Ultrasonics Symposium (IUS)
Glasgow, Scotland, October 6-9, 2019

Do raw signal data provide better localisation than image data for super-resolution imaging?

Konstantinos Diamantis
Institute for Digital Communications
University of Edinburgh
Edinburgh, UK
K.Diamantis@ed.ac.uk

Tom Anderson
Centre for Cardiovascular Science
The University of Edinburgh
Edinburgh, UK
tanders1@exseed.ed.ac.uk

Paul Dalgarno
School of Engineering and Physical Sciences
Heriot-Watt University
Edinburgh, UK
p.a.dalgarno@hw.ac.uk

Jørgen Arendt Jensen
Center for Fast Ultrasound Imaging
Technical University of Denmark
Lyngby , Denmark
jaj@elektro.dtu.dk

Vassilis Sboros
School of Engineering and Physical Sciences
Heriot-Watt University
Edinburgh, UK
V.Sboros@hw.ac.uk

***Abstract*— Super-resolution ultrasound imaging has evolved using image analysis algorithms. However, the images used are not generated with beamformers that are designed for single particle imaging, but rather for anatomy that provide continuous features (eg. delay and sum). In order to compare image- and signal-derived localisation accuracies we used multi-focal imaging combined with the simple metric of sharpness. A 7 MHz (λ=212 µm) linear array with 192 elements is used to scan a phantom that is composed of a thin wire. The average axial localisation accuracy using the sharpness method on the raw signal is ≈ 0.01λ while the centre of mass best measurement on image data provided ≈ 0.06λ. It is concluded that image derived localisation is compromised by the process that generates the image. It is therefore suggested that super-resolution imaging will benefit from alternative beamforming methods that are designed to enhance single particle imaging.**

Keywords*— *Axial localisation, beamforming, multiple focusing, microbubble, normalised sharpness, ultrasound imaging

I. INTRODUCTION

In ultrasound imaging, the interference of emitted wavefronts reduce the focusing capability of an aperture. Small objects can be resolved as in all wavefront based sensing methods, only to the diffraction limit and in combination with the duration of transmitted pulses. Super-resolution techniques are well-developed in other fields of sensing [1] including radar [2], astronomy [3], and optical microscopy [4]. Sub-diffraction ultrasound imaging is based on the utilization of contrast microbubbles due to their high scattering cross-section [5]. Subsequently, and as microbubbles travel within the vascular bed, super-resolution images of vascular structure has been made possible providing at least one order of magnitude resolution gains [6-8]. However, the image formation used in ultrasound equipment is designed for structural/anatomical imaging. The ultrasound super-resolution techniques above are applied to already beamformed images. The highly variable PSF, the noise, and a number of artefacts encountered in the ultrasound image may limit the final resolution.

Thus, it is important to investigate the performance of super-resolution methods that utilize raw data and compare these with derivations that originate from image data. The current paper investigates this using a sharpness derived methodology [9-12].

II. METHODS

The metric of image sharpness can be seen as a descriptor of field aberration. It maximizes at minimal aberration, and since it is dominated by defocus, it presents increasingly lower values with increasing defocus. A simplified version of the sharpness metric is calculated from a small region of interest (ROI) including the main-lobe of a single PSF, by:

$$S = \sum_{q=1}^{Q} E_q^4 / \left(\sum_{q=1}^{Q} E_q^2\right)^2 \qquad (1)$$

where S is the normalised ultrasound sharpness measured from the squared envelope detected data amplitudes Eq^2 (signal-derived sharpness), of Q samples (q = 1, . . . , Q). Alternatively the sharpness can be measured from the recorded pixel intensities of the saved images (image-derived sharpness), where the intensity of each pixel is proportional to the squared envelope amplitude. The region of interest (ROI) for these calculations in both cases is effectively a box around the PSF centre.

The processing methodology is detailed in [9]. The beamforming used is that of simple delay and sum with a single receive focus. The data are processed three times for three different receive foci. The calculation of sharpness at each depth and for each scatterer position results in overlayed 'sharpness curves' as shown in Fig.1. The depth estimation uses this result in order to estimate depth in an inverse process.

This work was supported by the Science and Technology Facilities Council (STFC-ST/M007804/1).

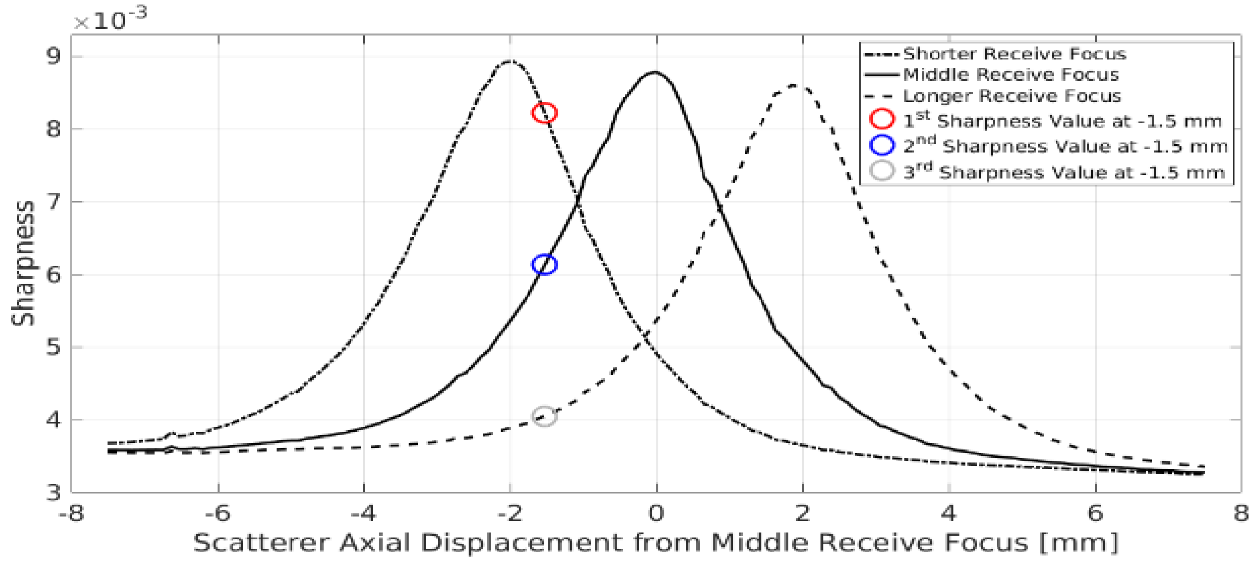

Fig. 1. Normalised Sharpness is plotted from all positions using the three foci. The sharpness is linked with axial position, and a single value would give an ambiguous dissemination of position. The 3 sharpness measures for a single axial position (a typical example is shown with the 3 circles at −1.5 mm) are combined into a maximum-likelihood function that derives the scatterer position with high accuracy.

The calculation of three sharpness values from each point source is fed into a maximum likelihood estimator [13] which then provides an output in the form of a probability density function that its maximum value is the axial location of a single point source. The accuracy of the normalised sharpness method is equivalent to the depth deviation of the method's z-estimate to the known scatterer position, or d_{dev} in short.

For the experimental verification the wire phantom setup in [9] was used. Briefly, a metal wire with 0.07 mm diameter was clamped inside a water tank and its axial movement was controlled by a positioning setup (AIMS III, Onda Corporation, Sunnyvale, CA). The ultrasound data were captured by the 1024 channel experimental ultrasound scanner SARUS (Synthetic Aperture Real-time Ultrasound System) [14] and using a BK8804 linear array (BK Ultrasound, Herlev, Denmark). Plane wave transmission was performed and RF data from one unfocused emission were acquired in receive. For each acquisition the data were beamformed in three different foci at 38 mm, 40 mm, and 42 mm.

In order to compare the results the commonly used centre of mass (COM) approach was used on the generated images and using the standard Matlab (The MathWorks, Inc., Natick, MA, USA) function *regionprops*.

III. Results

In Fig. 1, the measured mean sharpness was plotted over axial displacement for the RF data, corresponding to the left side y-axis. The RF data and image derived depth deviation are overlayed on the same figure and the respective y-axis text is on the right side. The image-derived sharpness processing resulted in an average d_{dev} that varied between 22.2±17.3μm (~0.10λ) and 26.3±22.7μm (~0.12 λ), depending on the depth range that was being examined. The displacement edges where the uncertainty of the measured sharpness becomes higher, are usually excluded from all the average d_{dev} calculations. These were improved by a factor of ~10 for the signal derived sharpness processing. The d_{dev} varied to between 2.3±1.8μm and 2.6±2.1μm (~0.01 λ). The COM provided a d_{dev} that ranged between 13.3±6.7μm (~0.06 λ) and 14.2±8.2μm (~0.07 λ). These numbers were an almost 2-fold improvement compared to those provided by the image-based sharpness. On the other hand, the COM based axial localisation was outperformed by the signal-derived sharpness processing by at least a factor of 6.5. Note, that the COM calculation was threshold dependent. Increasing or reducing the intensity threshold resulted in reduced localisation accuracy that reached values up to 44 μm (or ~0.207 λ). Fig. 2 shows how the three measurements vary across the depth that is covered by the three sharpness curves. Overall, the d_{dev} values were similar to those derived by the simulations [10].

IV. Discussion

The sharpness method provides consistently improved axial localisation precision, which is at least 2 orders of magnitude compared to the wavelength used (220 μm). Here, the raw data derived provided a near 10-fold improvement in axial localisation accuracy compared to the image derived data. The image formation includes compression, interpolation, time-gain compensation and display conversion which may contribute to loss of information. This explains the superiority of the signal-derived sharpness processing in axial localisation accuracy compared to the COM localisation by at least 5 times.

The normalised sharpness method, similar to the techniques that improve lateral [15,16] resolution, may add to the existing super-resolution methods. Current super-resolution ultrasound

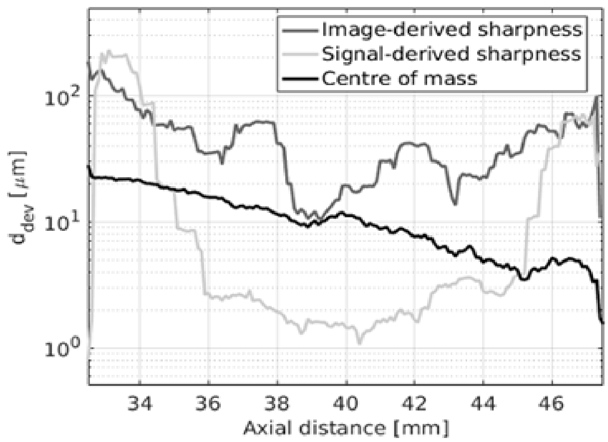

Fig. 2 Depth deviation to true simulated scatterer position (d_{dev}) plotted over axial distance for image- and signal-derived sharpness-based axial localization. The equivalent result of COM-based axial localization is also included.

is heavily based on image processing. It has been accomplished either by identifying the PSF COM [17], [18] or by fitting three dimensional Gaussian functions [3], [19] to ultrasound reconstructed data to approximate the PSF. Note that both methods provide similar results and are dependent on the SNR. Given that current imaging is not designed to enhance point scatter localisation, the sharpness method, although limited to the axial direction, may be a signal-based approach that may provide a new type of image data that are specifically designed for point scatter localisation and that can work well as an adjunct to the already existing image based methods.

V. Conclusion

Sharpness-based localisation is an alternative to classic image processing techniques for scatterer localisation in the axial direction. It was explained that the sharpness-based method predicts a depth estimate and its difference from the true scatterer position demonstrates its accuracy. The method can be implemented both using image and signal data with the signal-based implementation outperforming the image-based one or the conventional center of mass localisation which is also image-based. Changes in the scan grid while saving log-compressed ultrasound images and other intermediate processes prior to image formation alter the original signal information and compromise the overall performance of the method when using image data. Such details may be significant when reconstructing micro-vessels of the order of tens of micrometres in diameter.

References

[1] S. Haykin, J. H. Justice, N. L. Owsley, J. L. Yen, and A. C. Kak, Array signal processing. Englewood Cliffs, NJ: Prentice Hall, 1985.

[2] Quinquis, E. Radoi, and F. C. Totir, "Some radar imagery results using superresolution techniques," IEEE Trans. Antennas. & Propagation, vol. 52, no. 5, pp. 1–15, May 2004.

[3] K. G. Puschmann and F. Kneer, "On super-resolution in astronomical imaging," Astronomy & Astrophysics, vol. 436, no. 1, pp. 373–378, 2005

[4] M. Bates, B. Huang, G. T. Dempsey, and X. Zhuang, "Multicolor super-resolution imaging with photo-switchable fluorescent probes," Science, vol. 317, no. 5845, pp. 1749–1753, 2007.

[5] V. Sboros, C. M. Moran, S. D. Pye, and W. N. McDicken, "The behaviour of individual contrast agent microbubbles," Ultr. Med. Biol., vol. 29, no. 5, pp. 687–694, 2003.

[6] M. A. O'Reilly, R. M. Jones, and K. Hynynen, "Three-dimensional transcranial ultrasound imaging of microbubble clouds using a sparse hemispherical array," IEEE Trans. Biom. Eng., vol. 61, no. 4, pp. 1285–1294, 2014.

[7] K. Christensen-Jeffries, R. J. Browning, M. X. Tang, C. Dunsby, and R. J. Eckersley, "In vivo acoustic super-resolution and super-resolved velocity mapping using microbubbles," IEEE Trans. Medical Imaging, vol. 34, no. 2, pp. 433–440, Feb. 2015.

[8] O. Couture, B. Besson, G. Montaldo, M. Fink, and M. Tanter, "Microbubble ultrasound super-localisation imaging (MUSLI)," in Proc. IEEE Ultrason. Symp., 2011, pp. 1285–1287.

[9] K. Diamantis, A. Greenaway, T. Anderson, J. Jensen, P. Dalgarno, and V. Sboros, "Super-resolution axial localization of ultrasound scatter using multi-focal imaging," IEEE Trans. Biomed. Eng., vol. 65, no. 8, pp. 1840–1851, July 2018.

[10] K. Diamantis, T. Anderson, J. A. Jensen, P. A. Dalgarno, and V. Sboros, "Development of super-resolution sharpness-based axial localisation for ultrasound imaging," IEEE Access, vol. 7, pp. 6297–6309, 2019.

[11] K. Diamantis, P. A. Dalgarno, A. H. Greenaway, T. Anderson, J. A. Jensen, and V. Sboros, ''A novel array processing method for precise depth detection of ultrasound point scatter,'' in Proc. IEEE Int. Conf. Acoust., Speech, Signal Process. (ICASSP), Mar. 2016, pp. 669–673.

[12] K. Diamantis, P. A. Dalgarno, T. Anderson, J. A. Jensen and V. Sboros, "A comparison between image and signal sharpness-based axial localisation of ultrasound scatterers," *in Proc. IEEE 16th Int. Symp. on Biomed. Imag. (ISBI)*, Apr. 2019, pp. 1610-1613.

[13] H. I. C. Dalgarno, P. A. Dalgarno, A. C. Dada, G. J. G. C. E. Towers, R. M. Parton, I. Davis, R. J. Warburton, and A. H. Greenaway, "Nanometric depth resolution from multi-focal images in microscopy," J. R. Soc. Interface, vol. 8, no. 60, pp. 942–951, July 2011.

[14] J. A. Jensen, H. Holten-Lund, R. T. Nilsson, M. Hansen, U. D. Larsen, R. P. Domsten, B. G. Tomov, M. B. Stuart, S. I. Nikolov, M. J. Pihl, Y. Du, J. H. Rasmussen, and M. F. Rasmussen, "Sarus: A synthetic aperture real-time ultrasound system," IEEE Trans. Ultrason., Ferroelectr., Freq. Control, vol. 60, no. 9, pp. 1838-1852, 2013

[15] K. Diamantis, A. Greenaway, T. Anderson, J. A. Jensen, and V. Sboros, "Experimental performance assessment of the sub-band minimum variance beamformer for ultrasound imaging," Ultrasonics, vol. 79, pp. 87–95, 2017

[16] K. Diamantis, T. Anderson, M. B. Butler, C. A. Villag´omez-Hoyos, J. A.Jensen, and V. Sboros, "Resolving ultrasound contrast microbubbles using minimum variance beamforming," IEEE Trans. Med. Imag., vol. 38, no. 1, pp. 194–204, Jan. 2019.

[17] F. S. Foster, C. J. Pavlin, K. A. Harasiewicz, D. A. Christopher, and D. H. Turnbull, "Advances in ultrasound biomicroscopy," Ultr. Med Biol., vol. 26, no. 1, pp. 1–27, Jan. 2000.

[18] L. Pantoni, "Cerebral small vessel disease: From pathogenesis and clinical characteristics to therapeutic challenges," Lancet Neurol., vol. 9, no. 7, pp. 689–701, 2010

[19] S. T. Hess, T. P. K. Girirajan, and M. D. Mason, "Ultra-high resolution imaging by fluorescence photoactivation localisation microscopy," Biophys. J., vol. 91, no. 11, pp. 4258–4272, 2006.